ISBN: 978-3-95450-247-9 ISSN: 2673-5490 doi: 10.18429/JACoW-IPAC2024-TUPC65

CALCULATING THE CHANNELLING EFFICIENCY OF BENT SILICON CRYSTALS USING TWO PARTICLE SIMULATION PROGRAMS: SIXTRACK AND XSUITE

K. A. Dewhurst *, F. Van der Veken, P. D. Hermes, D. Mirarchi, S. Redaelli, CERN, Geneva, Switzerland

Abstract

A novel double-crystal experiment is being considered for installation in CERN's Large Hadron Collider (LHC) to measure precession properties of short-lived baryons such as the Λ_c^+. The experiment utilises a first bent silicon crystal of 50 µrad to deflect halo particles away from the circulating proton beam. Further downstream, a second crystal is installed, which produces a significantly greater bending angle of 7 mrad. While the former is well understood in simulations and measurements, the latter presents a new challenge for existing simulation tools. Using particle tracking programs, SixTrack and the newly developed Xsuite, we simulate a single pass experiment to calculate the expected channelling efficiency of these crystals. The results serve as a prediction for the performance of prototype crystals recently tested in CERN's North Experimental Area at 180 GeV, and that are planned to be installed in the LHC in 2025 for use in the multi-TeV energy range.

INTRODUCTION

As part of the Physics Beyond Colliders (PBC) studies at CERN [1], a fixed-target experiment using two bent crystals is being considered for installation in the Large Hadron Collider (LHC) [2, 3]. This experiment aims to measure the spin-precession properties (the electric- and magnetic-dipole moments) of short-lived Λ_c^+ baryons [4, 5]. The experiment incorporates two bent silicon crystals. The first crystal, the TCCS (Target Collimator Crystal for Splitting), will deflect LHC protons away from the main beam halo onto a tungsten target to produce Λ_c^+ baryons. The second crystal, the TCCP (Target Collimator Crystal for Precession), will be adjacent to the target, deflecting the produced Λ_c^+ particles and causing them to precess inside the crystal during their short lifetime of $\tau_{\Lambda_c^+} \approx 200$ fs [6] (at rest).

The TCCS is of the same type as the existing TCPC crystals installed as part of the LHC collimation system [7] with 4 mm length and 50 µrad bend angle. The crystal parameters are summarised in Table 1. The modelling of the TCCS with the simulation tool SixTrack [8] has been benchmarked against several crystal measurement studies at CERN [9–13], with convincing agreement between simulation and measurement. The TCCP is required to be considerably longer to cause significant precession before decay, e.g. 2 TeV ($\gamma \sim 2100$) Λ_c^+ baryons will travel ~ 120 mm in the experiment rest-frame before decaying. The TCCP is 70 mm long with a ~ 7 mrad bend angle to cause the required precession (equivalent to a ~ 6600 T m magnetic field).

* kay.dewhurst@cern.ch

SixTrack is a particle tracking code used and developed at CERN since 1994. It contains the Monte-Carlo routine *K2*, simulating the interaction of protons with matter, including physics specific to bent crystals [14–17]. Xsuite is being developed in Python and C, and is a successor to SixTrack with additional functionality. It removes reliance on legacy code in other languages (e.g. Fortran) and implements a modular format, allowing for more streamlined development and faster simulations [18]. The Xsuite crystal routine *Everest* is part of the Xcoll module and contains an updated methodology of the K2 crystal physics routine [19]. In K2, a crystal is considered as a thin element. In Everest, a crystal is a thick element where each particle will undergo a new interaction after a randomly sampled interaction length until the particle exits the crystal. Thus, Everest is capable of simulating multiple interactions, which is expected to provide more accurate simulations of particle channelling for the long TCCP crystal [20].

As the TCCS is short (4 mm) we expect both approaches to produce similar results. The longer (70 mm) TCCP crystal provides the opportunity to test and further benchmark the new simulation tool in Xsuite. Both the TCCS and TCCP have been recently tested (publication in preparation [21]) in single-pass experiments using the H8 beamline in the CERN North Experimental Area [22] to measure their channelling efficiencies. In this paper, we provide simulations from both SixTrack and Xsuite to predict the expected channelling efficiency for each crystal in these H8 experiments.

CRYSTAL CHANNELLING ROUTINE: XSUITE, EVEREST

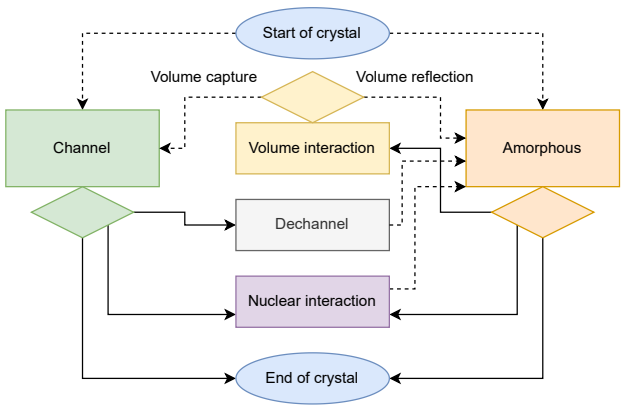

Figure 1: Logic of the Everest crystal routine in Xcoll. Solid arrows indicate the particle travels a distance (calculated path length) before the next interaction. Dashed arrows indicate the next process in the simulation without travel.

ISBN: 978-3-95450-247-9 ISSN: 2673-5490 doi: 10.18429/JACoW-IPAC2024-TUPC65

Table 1: Crystal Parameters

Crystal	Bend angle (specification [23])	Bend angle (simulated)	Length [mm]
TCCS	50 to 55 µrad	50 µrad	4
TCCP	6.0 to 7.5 mrad	6.9 mrad	70

When a charged particle enters a crystal, it may be captured between crystalline planes and channelled, or undergo amorphous (Coulomb) scattering [24]. In either case, the particle will travel some distance into the crystal before its next interaction with the crystal lattice. In Everest, for each potential crystal interaction (e.g. nuclear interaction, dechannelling, volume interaction, exiting the crystal) [24] a path length is determined from random sampling of a probability function. The shortest path is taken by the particle, and the corresponding most probable interaction is assumed to take place. The process repeats until the end of the crystal is reached. A flowchart of the Everest crystal routine logic is shown in Figure 1. In the case of short crystals, only one interaction calculation may occur.

CHANNELLING EFFICIENCY: SINGLE PASS EXPERIMENT

Charged particles that enter a silicon crystal with a suitable energy and incoming angle can be captured in the potential well between the crystalline planes and channelled [24]. Particles with the potential to be channelled by a bent crystal, enter within a critical angle [24]

$$\theta_{crit} = \left(1 - \frac{\rho_{crit}}{\rho}\right)\sqrt{\frac{2U}{E}}, \tag{1}$$

that depends on bending radius ρ of the crystal, the potential well depth U and the energy of the incoming particles E. A critical bending radius ρ_{crit} is defined from properties of the crystal lattice

$$\rho_{crit} = \frac{E}{2U}\left(\frac{d_p}{2} - a_{TF}\right), \tag{2}$$

where d_p is the inter-planar distance and a_{TF} is the screening length from the Thomas-Fermi atomic model [25].

To simulate the H8 single pass experiments, a Gaussian distribution of 1×10^7 particles was initialised in x, y, p_x, p_y (see Table 2) at the entrance of a crystal in the chosen simulation tool and compared to the distribution at the crystal exit. H8 can provide two beams that are utilised for crystal efficiency measurements; a 180 GeV pion beam and a 400 GeV proton beam (see Table 2). We consider particles impacting the crystal, that have angles within either $\pm\frac{1}{2}\theta_{crit}$ or $\pm\theta_{crit}$, and report the simulated channelling efficiency for each combination of crystal and beam in Tables 3 and 4.

SHORT CRYSTAL COMPARISON - TCCS

To calculate the channelling efficiency, the change in angle caused by the interaction with the crystal was plotted,

Table 2: Beam Distributions with Transverse Gaussian Profile

Particle	Energy	$\sigma_{x,y}$	$\sigma_{xp,yp}$
pion	180 GeV	2 mm	60 µrad
proton	400 GeV	1 mm	10 µrad

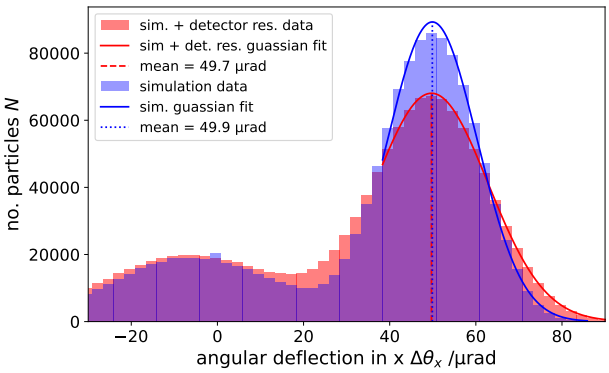

Figure 2: Angular deflection in x of 180 GeV particles for the TCCS crystal with data cut at $\pm\theta_{crit}$, where θ_{crit} = 13.3 µrad. Data from a SixTrack simulation with (red) and without (blue) the effect of the detector resolution. A Gaussian fit is made to the right side of the channelled peaks.

as in Figure 2. Channelled particles form a peak (right) around the bend angle of the crystal. Particles undergoing amorphous scattering have on average zero deflection and those undergoing volume reflection have a negative deflection angle; a combination of these two processes form a peak close to 0 µrad (left). Between the two peaks, the histogram is populated by dechannelled particles, i.e. those leaving channelling before the end of the crystal. The channelling efficiency is given by the proportion of channelled particles compared to the total particles suitable for channelling;

$$\epsilon_{ch}[\%] = \frac{\text{no. particles channelled}}{\text{total no. particles}} \times 100. \tag{3}$$

Table 3: Simulated TCCS Channelling Efficiency

Energy [GeV]	Cut [µrad]	Simulation tool	Channelling efficiency [%]
180	6.65	SixTrack	79.2 ± 0.2
	6.65	Xsuite	81.4 ± 0.3
	13.3	SixTrack	68.6 ± 0.2
	13.3	Xsuite	68.8 ± 0.2
400	4.45	SixTrack	77.2 ± 0.1
	4.45	Xsuite	79.1 ± 0.1
	8.9	SixTrack	69.2 ± 0.1
	8.9	Xsuite	69.9 ± 0.1

The number of channelled particles was estimated by performing a Gaussian fit mainly to the right side of the channelled peak to discount the background of dechannelled par-

ISBN: 978-3-95450-247-9 ISSN: 2673-5490 doi: 10.18429/JACoW-IPAC2024-TUPC65

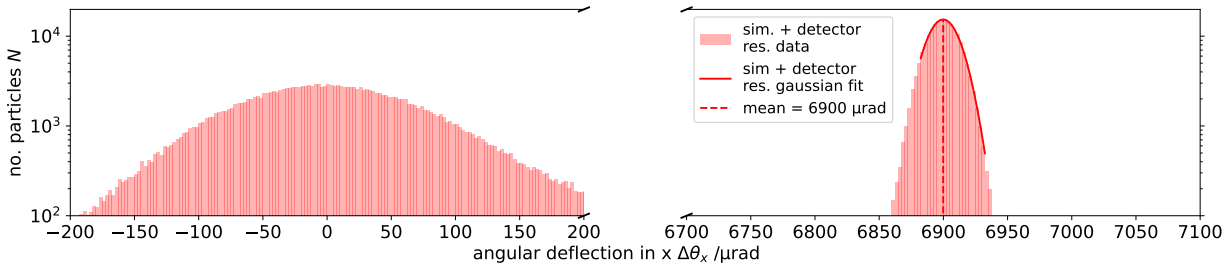

Figure 3: The angular deflection in x of 180 GeV particles for the TCCP crystal with data cut at the critical angle of 12.9 µrad (log scale on y-axis). Data from an Xsuite simulation is shown with the effect of the detector resolution. A Gaussian fit, made to the channelled peak, returns the expected bend angle of 6.9 mrad and gives a channelling efficiency $\epsilon_{ch} = 32 \pm 1$ %.

ticles. The fit parameters were used to calculate the number channelled particles enclosed by a full Gaussian.

To predict the data recorded in single-pass experiments, the detector resolution was included in the analysis. The telescope used in the 2023 measurement is expected to have a 3.5 µrad resolution for the incoming angle using silicon telescopes [26] and a 7.2 µrad resolution for the outgoing angle using a combination of a silicon telescope and a beam chamber [27] detector. To simulate the effect of the experiment resolution, a random noise signal (Gaussian with σ equal to the resolution) was added to the data for incoming and outgoing angle. Figure 2 shows the effect of the detector resolution. A simulation without the detector resolution (blue) gives a higher peak and larger estimate of $\epsilon_{ch} = 71$ %, whereas with a spread caused by the detector resolution (red), the measured efficiency is lower $\epsilon_{ch} = 69$ %. In both cases the Gaussian fit recovers the expected crystal bend angle of 50 µrad to the nearest µrad.

Propagation of statistical uncertainty, assuming $\sigma = \sqrt{N}$ on the height of each histogram bar, suggests < 0.5% uncertainty on the channelling efficiencies for the TCCS, as reported in Table 3. However, a larger uncertainty arises from the selection of data in the channelled-peak fit, e.g. varying the lower limit by ±4 µrad altered the channelling efficiency by ±1% for the TCCS. This larger uncertainty should be considered in comparisons with measurements. Table 3 summarises the channelling efficiencies for the TCCS with 180 GeV and 400 GeV particles and cuts at $\pm\frac{1}{2}\theta_{crit}$ and $\pm\theta_{crit}$. All values reported in Table 3 include the detector resolution. As expected, the results from both simulation tools SixTrack and Xsuite agree within a few percent.

LONG CRYSTAL COMPARISON - TCCP

The same approach to simulation and analysis was taken for the TCCP. Initial x-ray analysis suggests the manufactured TCCP has a bend angle of 6.9 mrad [28]; we used this value in our simulations.

Figure 3 shows the angular deflection of particles interacting with the TCCP in an Xsuite simulation. The amorphous and channelled peaks are well separated, and the background of dechannelled particles is low compared to the TCCS. The calculated channelling efficiencies are shown in Table 4. As expected, the TCCP has a lower efficiency than the TCCS,

Table 4: TCCP Channelling Efficiency

Energy [GeV]	Cut [µrad]	Simulation tool	Channelling efficiency [%]
180	6.45	SixTrack	36.6 ± 0.2
	6.45	Xsuite	37.4 ± 0.2
	12.9	SixTrack	30.9 ± 0.1
	12.9	Xsuite	31.2 ± 0.1
400	4.15	SixTrack	48.0 ± 0.1
	4.15	Xsuite	48.4 ± 0.1
	8.3	SixTrack	42.8 ± 0.1
	8.3	Xsuite	42.5 ± 0.1

as the smaller bend radius decreases the channelling potential well in the crystal and the greater length provides more opportunity for particles to dechannel. Surprisingly, there is little difference in channelling efficiency resulting from SixTrack and Xsuite simulations for the TCCP. The differences in the crystal physics routines do not seem to have a considerable impact for the chosen simulation setup. The simulations reported here assume a perfect crystal; well aligned to the incoming beam, with uniform bend radius, and no amorphous edge layer or miscut on the crystal face. The channelling efficiencies reported, therefore, provide an upper bound for the expected channelling efficiency from measurement of the real crystals.

CONCLUSION

Both the simulation tools SixTrack and Xsuite include crystal routines enabling them to track particles through bent silicon crystals. SixTrack assumes crystals as thin-elements, whereas Xsuite can take a thick-element approach for longer crystals. We have used both tools to simulate the single-pass channelling efficiency for two crystals; the 4 mm TCCS and 70 mm TCCP, which are considered for installation into the LHC for a fixed-target experiment. Both simulation tools produced similar predictions for the channelling efficiency, verifying that both are suitable tools for similar future studies. The results provide a useful upper-bound of the expected channelling efficiencies to compare with experimental measurements from the H8 beamline at CERN.

ISBN: 978-3-95450-247-9 ISSN: 2673-5490 doi: 10.18429/JACoW-IPAC2024-TUPC65

REFERENCES

[1] J. Jaeckel, M. Lamont, and C. Vallée, "The quest for new physics with the Physics Beyond Colliders programme," *Nat. Phys.*, vol. 16, no. 4, pp. 393–401, 2020. doi:10.1038/s41567-020-0838-4

[2] K. A. Dewhurst, M. D'Andrea, P. D. Hermes, D. Mirarchi, M. Patecki, and S. Redaelli, "Performance of a double-crystal setup for LHC fixed-target experiments," in *Proc. of the 14th Int. Particle Accelerator Conf.*, 2023, pp. 632–635. doi:10.18429/JACoW-IPAC2023-MOPL048

[3] K. A. Dewhurst *et al.*, "Design and layout of a double-crystal proof-of-principle experiment in the Large Hadron Collider," *unpublished*, 2024.

[4] F. J. Botella *et al.*, "On the search for the electric dipole moment of strange and charm baryons at LHC," *Eur. Phys. J. C*, vol. 77, no. 3, 181(1–15), 2017. doi:10.1140/epjc/s10052-017-4679-y

[5] V. M. Biryukov and J. Ruiz-Vidal, "Improved experimental layout for dipole moment measurements at the LHC," *Eur. Phys. J. C*, vol. 82, no. 2, p. 149, 2022. doi:10.1140/epjc/s10052-022-10114-5

[6] R. Aaij *et al.*, "Precision measurement of the Lambda(+)(c), Xi(+)(c), and Xi(0)(c) baryon lifetimes," *Phys. Rev. D*, vol. 100, no. 3, p. 032 001, 2019, (LHCb Collaboration). doi:10.1103/PhysRevD.100.032001

[7] M. D'Andrea *et al.*, "Characterization of bent crystals for beam collimation with 6.8 TeV proton beams at the LHC," *NIM-A*, p. 169 062, 2023. doi:10.1016/j.nima.2023.169062

[8] R. De Maria *et al.*, "SixTrack Version 5: Status and New Developments," in *Proc. of the 10th Int. Particle Accelerator Conf.*, 2019, pp. 3200–3203. doi:10.18429/JACOW-IPAC2019-WEPTS043

[9] D. Mirarchi, G. Hall, S. Redaelli, and W. Scandale, "A crystal routine for collimation studies in circular proton accelerators," *NIM-B*, vol. 355, pp. 378–382, 2015. doi:10.1016/j.nimb.2015.03.026

[10] W. Scandale *et al.*, "Observation of strong leakage reduction in crystal assisted collimation of the SPS beam," *Physics Letters B*, vol. 748, pp. 451–454, 2015. doi:10.1016/j.physletb.2015.07.040

[11] R. Rossi, "Experimental Assessment of Crystal Collimation at the Large Hadron Collider," Ph.D. dissertation, Rome U., 2017. http://cds.cern.ch/record/2644175

[12] W. Scandale *et al.*, "Study of inelastic nuclear interactions of 400 GeV/c protons in bent silicon crystals for beam steering purposes," *Eur. Phys. J. C*, vol. 78, no. 6, p. 505, 2018. doi:10.1140/epjc/s10052-018-5985-8

[13] D. Mirarchi *et al.*, "Reducing Beam-Related Background on Forward Physics Detectors Using Crystal Collimation at the Large Hadron Collider1," *Phys. Rev. Appl.*, vol. 14, no. 6, p. 064 066, 2020. doi:10.1103/PhysRevApplied.14.064066

[14] V. Previtali, Ed., *Performance Evaluation of a Crystal-Enhanced Collimation System for the LHC*. EPFL, 2010. doi:10.5075/epfl-thesis-4794

[15] S. Redaelli, Ed., *Proceedings of ICFA Mini-Workshop on Tracking for Collimation in Particle Accelerators: Oct 30, 2015*. CERN, 2018, vol. 2/2018. doi:10.23732/CYRCP-2018-002

[16] D. Mirarchi, S. Redaelli, and W. Scandale, "Crystal implementation in SixTrack for proton beams," *CERN Yellow Reports: Conference Proceedings*, pp. 91–108, 2018. doi:10.23732/CYRCP-2018-002.91

[17] M. D'Andrea, A. Mereghetti, D. Mirarchi, V. Olsen, and S. Redaelli, "Release of Crystal Routine for Multi-Turn Proton Simulations within SixTrack v5," in *Proc. of the 12th Int. Particle Accelerator Conf.*, 2021, pp. 2648–2651. doi:10.18429/JACoW-IPAC2021-WEPAB024

[18] G. Iadarola *et al.*, *Xsuite: An integrated beam physics simulation framework*, arXiv:2310.00317 [physics], 2023. doi:10.48550/arXiv.2310.00317

[19] D. Demetriadou, A. Abramov, G. Iadarola, and F. Van der Veken, "Tools for integrated simulation of collimation processes in Xsuite," in *Proc. of the 14th Int. Particle Accelerator Conf.*, 2023, pp. 2801–2804. doi:10.18429/JACOW-IPAC2023-WEPA066

[20] F. Van Der Veken *et al.*, "Recent Developments with the New Tools for Collimation Simulations in Xsuite," in *Proceedings of the 68th Adv. Beam Dyn. Workshop High-Intensity High-Brightness Hadron Beams*, 2024, p. 4. doi:doi:10.18429/JACoW-HB2023-THBP13

[21] S. Cesare *et al.*, "Performance of short and long bent crystals for the TWOCRYST experiment at the Large Hadron Collider (LHC)," *unpublished*, 2024.

[22] R. Rossi, G. Cavoto, D. Mirarchi, S. Redaelli, and W. Scandale, "Measurements of coherent interactions of 400 GeV protons in silicon bent crystals," *NIM-B*, vol. 355, pp. 369–373, 2015. doi:10.1016/j.nimb.2015.03.001

[23] Q. Demassieux *et al.*, *[TCCS/TCCP] Functional and Operational Conditions for the Double-Crystal setup in the LHC IR3*, Restricted access, 2022. https://edms.cern.ch/document/2742008/1.0

[24] V. M. Biryukov, Y. A. Chesnokov, and V. I. Kotov, *Crystal Channeling and Its Application at High-Energy Accelerators*, F. Bonaudi and C. W. Fabjan, Eds. Springer, 1997. doi:10.1007/978-3-662-03407-1

[25] Y. Yamamura, W. Takeuchi, and T. Kawamura, "The screening length of interatomic potential in atomic collisions," National Institution for Fusion Science, Tech. Rep. NIFS-DATA-45, 1998, INIS Reference Number: 29061312, p. 32. https://inis.iaea.org/collection/NCLCollectionStore/_Public/29/061/29061312.pdf

[26] D. Lietti, A. Berra, M. Prest, and E. Vallazza, "A microstrip silicon telescope for high performance particle tracking," *NIM-A*, vol. 729, pp. 527–536, 2013. doi:10.1016/j.nima.2013.07.066

[27] G. Barbiellini *et al.*, "The AGILE silicon tracker: Testbeam results of the prototype silicon detector," *NIM-A*, vol. 490, no. 1, pp. 146–158, 2002. doi:10.1016/S0168-9002(02)01062-8

[28] E. Matheson, *Crystal X-ray validation at CERN*, 2023. https://indico.ijclab.in2p3.fr/event/9924/timetable/#20231211.detailed